AD-A081 722 KAMAN AVIDYNE BURLINGTON MA F/G 20/4
THE VIBRA-8 SUBSONIC AERODYNAMIC NUCLEAR GUST VULNERABILITY COD--ETC(U)
MAY 79 G ZARTARIAN DNA001-78-C-0317
UNCLASSIFIED KA-TR-164 DNA-4966F NL

END
DATE FILMED
4-80
DTIC

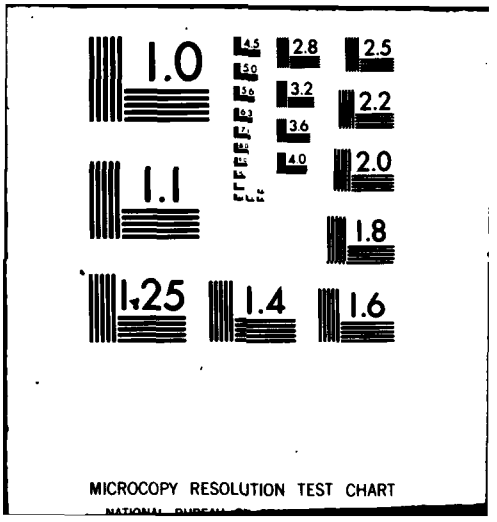
1.0
1.1
1.25
1.4
1.6
1.8
2.0
2.2
2.5
2.8
3.2
3.6
4.0
4.5
5.0
5.6
6.3
MICROCOPY RESOLUTION TEST CHART

(12) LEVEL III

DNA 4966F

THE VIBRA-8 SUBSONIC AERODYNAMIC NUCLEAR GUST VULNERABILITY CODE

Garabed Zartarian

Kaman AviDyne
83 Second Avenue
Burlington, Massachusetts 01803

1 May 1979

Final Report for Period July 1978—February 1979

CONTRACT No. DNA 001-78-C-0317

APPROVED FOR PUBLIC RELEASE;
DISTRIBUTION UNLIMITED.

THIS WORK SPONSORED BY THE DEFENSE NUCLEAR AGENCY
UNDER RDT&E RMSS CODE B340278464 N99QAXAJ50206 H2590D.

Prepared for
Director
DEFENSE NUCLEAR AGENCY
Washington, D. C. 20305

Destroy this report when it is no longer needed. Do not return to sender.

PLEASE NOTIFY THE DEFENSE NUCLEAR AGENCY, ATTN: STTI, WASHINGTON, D.C. 20305, IF YOUR ADDRESS IS INCORRECT, IF YOU WISH TO BE DELETED FROM THE DISTRIBUTION LIST, OR IF THE ADDRESSEE IS NO LONGER EMPLOYED BY YOUR ORGANIZATION.

6270411

(18) DNA, SBIE

UNCLASSIFIED

SECURITY CLASSIFICATION OF THIS PAGE (When Data Entered)

(19) REPORT DOCUMENTATION PAGE	READ INSTRUCTIONS BEFORE COMPLETING FORM
1. REPORT NUMBER: DNA 4966F / AD-E300 674	2. GOVT ACCESSION NO. / 3. RECIPIENT'S CATALOG NUMBER (9)
4. TITLE (and Subtitle): (6) THE VIBRA-8 SUBSONIC AERODYNAMIC NUCLEAR GUST VULNERABILITY CODE,	5. TYPE OF REPORT & PERIOD COVERED: Final Report for Period July 1978—February 1979 (13)
	6. PERFORMING ORG. REPORT NUMBER: KA-TR-164 (14)
7. AUTHOR(s): (5) Garabed Zartarian	8. CONTRACT OR GRANT NUMBER(s): (15) DNA 001-78-C-0317
9. PERFORMING ORGANIZATION NAME AND ADDRESS: Kaman AviDyne / 83 Second Avenue / Burlington, Massachusetts 01803	10. PROGRAM ELEMENT, PROJECT, TASK AREA & WORK UNIT NUMBERS: (16) Subtask N99QAXA502-06
11. CONTROLLING OFFICE NAME AND ADDRESS: Director / Defense Nuclear Agency / Washington, D.C. 20305	12. REPORT DATE: (11) 1 May 1979 / 13. NUMBER OF PAGES: 22
14. MONITORING AGENCY NAME & ADDRESS (if different from Controlling Office): (12) 22	15. SECURITY CLASS (of this report): UNCLASSIFIED (17) 350 / 15a. DECLASSIFICATION/DOWNGRADING SCHEDULE

16. DISTRIBUTION STATEMENT (of this Report)

Approved for public release; distribution unlimited.

17. DISTRIBUTION STATEMENT (of the abstract entered in Block 20, if different from Report)

18. SUPPLEMENTARY NOTES

This work sponsored by the Defense Nuclear Agency under RDT&E RMSS Code B340278464 N99QAXAJ50206 H2590D.

19. KEY WORDS (Continue on reverse side if necessary and identify by block number)

Blast Vulnerability
Nuclear Effects

20. ABSTRACT (Continue on reverse side if necessary and identify by block number)

This report describes certain modifications to the subsonic aerodynamic subroutine in the earlier versions of VIBRA to extend the applicability of the nuclear vulnerability code over broader ranges of Mach number, aspect ratio, and sweep angles. This modified version, designated as VIBRA-8, was developed in conjunction with a study of the nuclear vulnerability of an aeronautical system. A separate classified report has been issued to cover that study.

DD FORM 1 JAN 73 1473 EDITION OF 1 NOV 65 IS OBSOLETE

UNCLASSIFIED

SECURITY CLASSIFICATION OF THIS PAGE (When Data Entered)

L7497C

PREFACE

This report was prepared by Kaman AviDyne, a Division of Kaman Sciences Corporation, Burlington, Massachusetts, for the Defense Nuclear Agency, as part of the total effort under Contract No. DNA001-78-C-0317. The work was performed within the Structural Mechanics Group, headed by Mr. Emanuel S. Criscione. Captain Michael Rafferty of DNA was the Technical Monitor.

The author wishes to express his appreciation to Dr. Norman P. Hobbs, the Technical Director at Kaman AviDyne, who reviewed this effort and directed the KA programming staff in implementing the necessary changes in the affected subroutine of the VIBRA code.

A MODIFIED SUBSONIC AERODYNAMIC SUBROUTINE FOR THE VIBRA NUCLEAR VULNERABILITY CODE

1. INTRODUCTION.

The aerodynamic subroutine in VIBRA-4 (Reference 1) for lifting surfaces of aircraft flying at subsonic speeds was devised from empirical results. For all practical purposes, this subroutine is essentially the same as that in the earlier VIBRA versions. Prepared nearly twenty years ago, the original version (Reference 2) was tailored specifically for configurations of interest at that time. The data utilized in Reference 2 consist of "average" values which are deemed acceptable whenever the Mach number (M) is around 0.8, the aspect ratio (AR) is between 4 and 6, and the quarter-chord sweep (Λ) is say between 35 and 45 degrees. Some current aeronautical systems have higher aspect ratios, lower sweeps, and the flight speeds are such that M falls between 0.5 and 0.75.

In what follows, certain practical modifications are effected which allow the subsonic aerodynamic subroutine to be applicable over broader ranges of Mach number, aspect ratio, and sweep; and, more specifically, over the ranges $0.5 \leq M \leq 0.8$, $3 \leq AR \leq 12$, and $0 \leq \Lambda \leq 60$ degrees. The latest VIBRA version, designated as VIBRA-8, differs from VIBRA-4 in that it includes the modified and improved subsonic aerodynamic subroutine. Section II of the original VIBRA report (Reference 2), which documents the subsonic formulation for all versions through VIBRA-4, is followed in the discussions below. The intent of this short report is to justify and to document the effected modifications and additions.

2. AERODYNAMIC CONSIDERATIONS.

There are three areas which need to be examined:

1. Potential flow results for the ratio of two-dimensional normal force coefficient to angle of attack as a function of aerodynamic time.

2. Two-dimensional, non-potential flow, large angle of attack effects.

3. Three-dimensional effects.

2-1 Ratio of Two-Dimensional Normal Force Coefficient to Angle of Attack as a Function of Aerodynamic Time.

Consider first the function f(s),

$$f(s) = \frac{c_n(\alpha,s)}{\alpha} \quad , \tag{1}$$

which is the ratio of the normal force coefficient to angle of attack according to linearized potential flow theory for a two-dimensional unswept wing subjected to a step change in angle of attack, i.e., the indicial problem. This functionality with respect to the dimensionless time parameter s is given by Eq. (128) and Figure 9 in Reference 2, with the units of f(s) being per degree. The value of f(s) according to Eq. (128) should be related to the so-called Wagner function, ϕ_c, as given on Page 350 of Reference 3. In fact, it can be easily shown that

$$f(s) = 2\pi\phi_c(s) \tag{2a}$$

if f(s) is expressed in units of per radian, and

$$f(s) \equiv \frac{\pi^2}{90}\phi_c(s) \tag{2b}$$

if f(s) is expressed in units of per degree.

Invariably, the function ϕ_c is approximated in practical applications through the expression

$$\phi_c(s) = b_0 + b_1e^{-2\beta_1 s} + b_2e^{-2\beta_2 s} + b_3e^{-2\beta_3 s} \tag{3}$$

where $b_0,\ldots b_3$, $\beta_1\ldots,\beta_3$ are parameters depending on Mach number only. This expression differs slightly from the corresponding one in Reference 3. The adjustment here is due to the fact that in Reference 3 the parameter s=Ut/c, whereas in Reference 2 and here s=2Ut/c, where U is the wind speed, t is time, and c is the chord.

From steady-state considerations for an unswept two-dimensional (2D) airfoil in subsonic compressible flow,

$$\frac{c_n(s=\infty)}{\alpha} = f(s=\infty) = \frac{2\pi}{\sqrt{1-M^2}} \tag{4}$$

It is also known that β_1, β_2, β_3 are always positive; and thus terms involving them $\to 0$ as $s \to \infty$. From Eq. (4) and Eq. (2a),

$$\phi_c(s\to\infty) = b_0 = \frac{1}{\sqrt{1-M^2}} \tag{5}$$

From acoustic theory (or linearized piston theory), the condition that the loading at t=s=0 depends on the instantaneous angle of attack, and more precisely,

$$\frac{c_n(s=0)}{\alpha} = f(s=0) = \frac{4}{M} \qquad \text{(per radian)}$$

leads to the result that

$$\left(b_0 + b_1 + b_2 + b_3\right) \text{must equal to } \frac{2}{\pi M},$$

or equivalently,

$$b_3 = \frac{2}{\pi M} - \frac{1}{\sqrt{1-M^2}} - b_1 - b_2 \tag{6}$$

except at M=0*. The entries in Table 6-1 of Reference 3 are in accord with the above results.

To avoid confusion in later derivations, quantities obtained from potential flow theory are so designated by a superscript P. Thus, when expressed in units of per degree,

$$f^P(s) = \left[\frac{c_n}{\alpha}(s,\alpha\to 0)\right]^P$$

$$= \frac{\pi^2}{90}\left(b_0 + b_1 e^{-2\beta_1 s} + b_2 e^{-2\beta_2 s} + b_3 e^{-2\beta_2 s}\right) \tag{7}$$

---

*When M=0, one has to deal with an impulse due to apparent mass effects.

It should be noted that f(s) as given by Equation (128) of the VIBRA report is really $f^P(s)$; and, as far as can be determined, it was obtained from data for a single Mach number, namely M=0.8. The first task at hand is to give formulas for $b_0,\ldots,\beta_3$ as functions of M, so that the more general equation (i.e., Eq. (7) above instead of Eq. (128)) may be applied to represent $f^P(s)$ for a range of Mach numbers, and not be limited to the single M=0.8. Using the numerical values from Table 6-1 of Reference 3 and corresponding values for M=0.8 from Reference 4, curves were fitted for each of the parameters $b_0,\ldots,\beta_3$. The curve fits resulted in the following expressions for the range $0.2 \leq M \leq 0.8$

$$
\begin{aligned}
b_o &= \frac{1}{\sqrt{1-M^2}} \\
b_1 &= -0.165 - 0.482M && 0.2 \leq M < 0.5 \\
&= 1.044 - 6.933333M + 11.4M^2 - 6.666667M^3 && 0.5 \leq M \leq 0.8 \\
b_2 &= -0.249 - 0.344\,(0.5 - M)^2 && 0.2 \leq M < 0.5 \\
&= 36.806 - 173.393M + 266.4M^2 - 135.668M^3 && 0.5 \leq M \leq 0.8 \\
b_3 &= \frac{2}{\pi M} - b_0 - b_1 - b_2 \\
\beta_1 &= 0.0754 - 0.1196\,(0.5 - M)^2 && 0.2 \leq M < 0.5 \\
&= 0.4029 - 1.50583M + 2.36M^2 - 1.31667M^3 && 0.5 \leq M \leq 0.8 \\
\beta_2 &= 0.300 + 0.288M^2 && 0.2 \leq M \leq 0.5 \\
&= -13.293 + 62.94667M - 94.15M^2 + 45.83333M^3 && 0.5 \leq M \leq 0.8 \\
\beta_3 &= 0.945M^{-1} && 0.2 \leq M \leq 0.5 \\
&= 58.96 - 257.59M + 380.4M^2 - 187.0M^3 && 0.5 \leq M \leq 0.8 \qquad (8)
\end{aligned}
$$

Through extensive calculations, it has been determined that when Eq. (7) is applied using the curve fitting expressions (Eq. (8)) considerable improvements are achieved in estimating $f^P(s)$; this is true even at the single Mach number (=0.8) for which Eq. (128) of Reference 2 was offered earlier.

Based on the above brief discussions, the following change was made:

Change 1:

(a) Omit Equation (128) of Reference 2.

(b) To replace it, compute first $b_0,\ldots,\beta_3$ according to Eq. (8) for the actual M.

(c) Use the $b_0,\ldots,\beta_3$ coefficients thus computed to find

$$f^P(s) = \frac{\pi^2}{90}\left\{b_0 + b_1 e^{-2\beta_1 s} + b_2 e^{-2\beta_2 s} + b_3 e^{-2\beta_3 s}\right\} \qquad (9)$$

which is in units of <u>per degree</u> and ready to replace Eq. (128). This eliminates the use of the <u>same</u> and less accurate formula for all subsonic M's.

2-2 Two Dimensional, Non-Potential Flow, Large Angle of Attack Effects.

Refer once more to Figure 9 of Reference 2. If the loadings were linear with angle of attack, the $f^P(s)$ as modified above would suffice for the two-dimensional case. However, <u>steady-state</u> measurements on airfoils show than $\frac{c_n}{\alpha}$ ($s\to\infty$, $\alpha\neq 0$) depends on α. This is evident from the asymptotes (i.e., as s → large values) of the non-potential curves in Figure 9. The non-potential conditions will henceforth be referred to as the NP-conditions; and to stress them, when necessary to do so for the sake of clarity, related quantities will be superscripted with NP.

As seen in the figure, the potential flow conditions prevail up to times $s=s_b(\alpha)$; thereafter, the curves decay towards their steady-state values as $s\to\infty$. Equation 129 of Reference 2 gives $f^{NP}(s)$ in the form

$$f^{NP}(s) = A_A + B_A e^{-C_A s} \qquad (10)$$

where A_A, B_A, and C_A are functions of α. Table I of the same reference gives the variations of A_A, B_A, and C_A with α. Presumably, these have been obtained from shock tube data and correspond to M=0.8. This $f^{NP}(s)$

is used for $s > s_b$ in previous VIBRA versions. Equation (10) needs to be reexamined. Let it be cast into the form

$$f^{NP}(s) = A_A\left(1 + \frac{B_A}{A_A} e^{-C_A s}\right)$$

$$= \left(A_A(\alpha=0)\right)\left(\frac{A_A(\alpha\neq 0)}{A_A(\alpha=0)}\right)\left(1 + \frac{B_A}{A_A} e^{-C_A s}\right) \qquad (11)$$

The first factor on the right hand side, i.e., $A_A(\alpha=0)$, is of special significance. The quantity $\frac{\pi A_A(\alpha=0)}{180}$ which is $A_A(\alpha=0)$ of Table I, but in units of per degree rather than per radian, is really $(c_n/\alpha)^P$, steady-state. Based on potential flow derivations in Reference 3,

$$\left(\frac{c_n}{\alpha}\right)^P_{\text{steady-state}} = \frac{\pi}{180} \cdot 2\pi b_0 = \frac{\pi^2}{90} \frac{1}{\sqrt{1-M^2}}$$

which is equal to 0.1828 for M=0.8. The entry $A_A(\alpha=0)$ in Table I gives for the same quantity the close value of 0.1837. Thus, an analytical expression has been established for $A_A(\alpha=0,M)$,

$$A_A(\alpha=0,\ M) = \frac{\pi^2}{90} \frac{1}{\sqrt{1-M^2}} \qquad \textit{(per degree)} \qquad (12)$$

which is no longer restricted to Mach numbers near 0.8.

Attention is next focused on the second term which is the ratio

$$r(\alpha) \equiv r = \frac{A_A(\alpha\neq 0)}{A_A(\alpha=0)} \qquad (13)$$

Note that $f^{NP}(s\to\infty) = A_A(\alpha\neq 0) = (A_A(\alpha=0))\ r$. From Table I, Reference 2, the following values are obtained for $r(\alpha,\ M=0.8)$:

α(deg)	$r(\alpha,\ M=0.8)$
0	1.0
5	0.6984
10	0.4573
15	0.3059
30	0.2559
45	0.2243
60	0.1998

A test was made to find out if this "distribution function" r fits experimental data at other Mach numbers. Had this test shown a reasonable fit, one could then use the above r-entries along with $A_A(\alpha=0, M)$ as given by Eq. (12) to obtain $f^{NP}(s\to\infty)$. Data for the symmetric 64A006 and 64A010 airfoils (6 and 10 percent thick, respectively) presented in Reference 5 were found suitable for this purpose. If one plots the experimental data for $r = \frac{(c_n/\alpha)_{\alpha\neq 0}}{(c_n/\alpha)_{\alpha=0}}$ versus α, and corresponding to M=0.3, 0.5, 0.7, and 0.8, the various M-curves do not fall close to each other. However, if one plots this ratio r as a function of α_e, where α_e is the "equivalent angle of attack at M=0.8"

$$\alpha_e = \frac{0.6\alpha}{\sqrt{1-M^2}},$$

then all the data points fall close to an "average curve". Since at M=0.8, $\alpha_e=\alpha$, this average curve should correspond to $r(\alpha=\alpha_e, M=0.8)$ and more or less duplicate the curve one has from the $r(\alpha, M=0.8)$-tabulation above, i.e., from Table I of Reference 2. There are some differences however. The average curve resulting from the steady-state data of Reference 5 is better defined and is therefore used here.

The above observations indicate that the dependency of r on two parameters α and M can be reduced to a dependency on the single parameter α_e. Thus,

$$r(\alpha,M) = r(\alpha_e)$$

from which it follows that

$$\begin{aligned} A_A(\alpha,M) &= A_A(\alpha=0, M)\ r\ (\alpha,M) \\ &= A_A(\alpha=0, M)\ r\ (\alpha_e) \\ &= r(\alpha_e)\ \frac{\pi^2}{90}\ \frac{1}{\sqrt{1-M^2}} \end{aligned} \qquad (14)$$

The average curve representing $r(\alpha_e)$ vs α_e and referred to earlier is described by the following table:

α_e(deg)	$r(\alpha_e)$ from "Average Curve"
0	1.0
±5	0.875
±10	0.440
±15	0.310
±30	0.256
±45	0.224
±90	0.151

Linear interpolation may be used for α_e's between the tabulated values. This table should be compared with the preceding $r(\alpha, M=0.8)$-tabulation.

Consider next the third factor on the right hand side of Eq. (11). One way of handling this "decay" is to assume that the non-potential value f^{NP} breaks from the potential value at the breakpoint $s=s_b(\alpha)$, where s_b's are as in the previous VIBRA versions, and that the decay is such that following 30 chord lengths of travel, i.e., at $s=s_b + 30$, the decay to the steady-state value $f^{NP}(\alpha, s\to\infty)$ is 99% complete. However, this is at most a rough approximation. One would do just as well to retain the previous f^{NP}-format, i.e.,

$$f^{NP} = A_A + B_A e^{-C_A s}$$

using $B_A = B_A(\alpha, M=0.8)$ and $C_A = C_A(\alpha, M=0.8)$ as given in Table I of Reference 2. (Of course, it may be argued that perhaps a better approach would be to say $B_A = B_A(\alpha_e)$ and $C_A = C_A(\alpha_e)$, in analogy with the change associated with $A_A(\alpha, M)$, i.e., Eq. (14). But there is no applicable data to support this hypothesis.)

Based on the above discussions, the following change was made:

Change 2:

(a) Use Eq. (129) of Reference 2, but with A_A (per radian) from Table I of the same reference replaced by

$$A_A(\alpha,M) = r(\alpha_e)\frac{2\pi}{\sqrt{1-M^2}} \quad \text{(units here are per radian)}$$

to obtain f^{NP}.

(b) Proceed in exactly the same manner as before, but with the modified f^{P} (Change 1) and f^{NP} (Change 2a), to obtain $\frac{c_n}{\alpha}$ (s,α).

2-3 Three-Dimensional Effects.

Attention is next turned to methods for accounting for three-dimensional (3D) and sweep effects. Consider first the steady-state case which corresponds to $s\to\infty$.

Figure 10A of Reference 2 gives the ratio $\frac{C_N}{c_n}$ $(\alpha,s\to\infty)$ as a function of α for a "representative case", namely that for M = 0.8, Λ = 35 to 45 deg, AR = 4 to 6. Of course, M, AR, and Λ are expected to affect this curve. One can see this by examining the <u>starting point</u>, i.e., $\frac{C_N}{c_n}$ $(\alpha=0,\ s\to\infty)$. Experimental data from a NASA Memorandum (Reference 6) have been used to confirm the well-known expression given as Eq. 6-35 in Reference 3 to be quite accurate. This expression (for the normal force slope) is:

$$C_{N_\alpha} = \frac{a_o \cos\Lambda_e}{\sqrt{1-M^2}} \cdot \frac{AR\sqrt{1-M^2}}{AR\sqrt{1-M^2}\sqrt{1+\left(\frac{a_o\cos\Lambda_e}{\pi AR\sqrt{1-M^2}}\right)^2}+\frac{a_o\cos\Lambda_e}{\pi}} \qquad (15)$$

where

$$\Lambda_e = \tan^{-1}\left(\frac{\tan\Lambda}{\sqrt{1-M^2}}\right) \qquad (15a)$$

The 2D <u>incompressible</u> lift curve slope a_o may be taken equal to 2π, and its compressible counterpart $c_{n_\alpha} = \frac{a_o}{\sqrt{1-M^2}} = \frac{2\pi}{\sqrt{1-M^2}}$.

Since

$$\frac{C_N}{c_n}(\alpha=0,\ s\to\infty) = \frac{C_{N_\alpha}}{c_{n_\alpha}},$$

one has from Eq. (15)

$$\frac{C_N}{c_n}(\alpha=0,\ s\to\infty) = \cos\Lambda_e\left(\frac{AR\sqrt{1-M^2}}{AR\sqrt{1-M^2}\sqrt{1+\left(\frac{2\cos\Lambda_e}{AR\sqrt{1-M^2}}\right)^2}+2\cos\Lambda_e}\right) \qquad (16)$$

Calculations for $\frac{C_N}{c_n}$ (α=0, s$\to\infty$) according to Eq. (16) show large variations with respect to M, Λ, and AR. The single representative value from Figure 10A of Reference 2 is around 0.445 (corresponding to M=0.8, Λ = 35 deg, AR = 5.5). But this ratio is substantially higher in cruise missile applications where one usually has lower M's, lower Λ's, and higher AR's. This indicates that Figure 10A must be adjusted to reflect its dependency on M, Λ, and AR.

Although the steady-state values of $\frac{C_N}{c_n}$ at $\underline{\alpha=0}$ for different (M, Λ, AR) combinations can be estimated adequately by the use of Eq. (16), the question still remains as to how to predict the variation of $\frac{C_N}{c_n}$ (α; M, Λ, AR) versus α. After much exploration, the following approximation was found to be in reasonable agreement with data used in the earlier VIBRA work <u>and</u> with related data from the NASA Memorandum (Reference 6):

$$\left.\begin{aligned} \frac{C_N}{c_n}(\alpha,\ s\to\infty;\ M,\Lambda,\ AR) &= \xi\ [1.7-0.7\cos 10\alpha_e] && 0 \le \alpha_e \le 18 \text{ deg} \\ &= \xi\ [2.05-0.35\cos 10\alpha_e] && 18 \le \alpha_e \le 36 \text{ deg} \\ &= \xi\ [1.7] && \alpha_e \ge 36 \text{ deg} \end{aligned}\right\} \quad (17)$$

where $\alpha_e = 0.6\alpha/\sqrt{1-M^2}$ as before, and

$\xi = \frac{C_N}{c_n}$ (α=0, s$\to\infty$; M, Λ, AR)

which is exactly the quantity obtained from Eq. (16).

Up to this point, one can get the 2D $c_n(\alpha,\ s\to\infty)$ and the 3D $C_N(\alpha,\ s\to\infty)$; but the C_N-value is for the total lifting surface. The next question to be addressed is how to distribute the load spanwise such that the total loading will correspond to C_N. A spanwise distribution, denoted by $g(\eta)$ (η being a dimensionless spanwise coordinate), is needed, such that the local <u>loading per unit span</u> is $\left\{g(\eta)C_N\right\}$.

In incompressible flow, the sectional lift $\ell(\eta)$ is elliptic if the chord varies elliptically along the span. If one sets

$$\ell(\eta) = qc(\eta)\, c_{\ell_\alpha}\, \alpha$$

and $c(\eta) = c_o\sqrt{1-\eta^2}$, where $\eta = |2y/\tilde{s}|$, $\tilde{s}$ = span, c_o = root chord, then at M=0, one would want c_{ℓ_α} = constant = k_o, i.e., independent of η.

Thus for an elliptic plan wing at M=0.

$$\ell(\eta) = qc_o\,(k_o\sqrt{1-\eta^2})\alpha$$

For non-elliptic wings at M=0, let

$$\ell(\eta) = qc_o\,\frac{k_o\sqrt{1-\eta^2}}{f(\eta)}\,\frac{c(\eta)}{c_o}\,\alpha \tag{18}$$

where $f(\eta)$ is to be chosen so that if the $c(\eta)$ becomes elliptic $f(\eta)$ cancels the $(c(\eta)/c_o)$-variation to give the $\sqrt{1-\eta^2}$ -type spanwise distribution. An elliptic wing may be thought of as approximately a tapered wing with taper ratio (TR) equal to

$$(TR)_e = \frac{\pi}{2} - 1 = 0.571$$

because its area is $\frac{\pi c_o \tilde{s}}{4}$ and the area of a tapered wing with root chord c_o and tip chord c_t is

$$\tilde{s}\left(\frac{c_t+c_o}{2}\right) = \tilde{s}c_o\left(\frac{1+(TR)}{2}\right).$$

A suitable expression for $f(\eta)$ is then

$$f(\eta) = 1 + ((TR)_e - 1)\eta = 1 - 0.429\eta$$

resulting in

$$\ell(\eta) = qc_o\left\{k_o\sqrt{1-\eta^2}\,\frac{1+(TR-1)\eta}{1-0.429\eta}\right\}\alpha \tag{19}$$

Equation (19) does not show the dependence of lift distribution on the effective sweep parameter $\Lambda_e = \tan^{-1}(\tan\Lambda/\sqrt{1-M^2})$ which is known to exist (e.g., Reference 7). (The Λ_e-parameter is the same as the commonly used Λ_β-parameter found in the same reference.) With no sweep, the sought distribution $g(\eta)$ is insensitive to M; but the magnitude of $\ell(\eta)$ is dependent on k_o which in turn depends on M through the factor

$1/\sqrt{1-M^2}$. Let Λ_e be given in degrees. Instead of using Eq. (19), a modified version would be more appropriate. Assuming the Λ_e-variation is a linear one, let

$$\ell(\eta) = qc_o \left\{ k_o \sqrt{1-\eta^2} \; \frac{1+(TR-1)\eta}{1-0.429\eta} \left(1 + a\eta^2 \; \frac{\Lambda_e}{45}\right) \right\} \alpha \qquad (20)$$

where "a" is a suitable constant to be determined through trial examples. Let further

$$I = \int_o^1 \sqrt{1-\eta^2} \left\{ \frac{1+(TR-1)\eta}{1-0.429\eta} \left(1 + a\eta^2 \; \frac{\Lambda_e}{45}\right) \right\} d\eta \qquad (21)$$

Then the total lift L is

$$L = 2\int_o^{\tilde{s}/2} \ell(y)dy = \tilde{s}\,(q)c_o k_o I\alpha$$

$$= \tilde{s}\, \frac{c_o+c_t}{2} \cdot \frac{2c_o}{c_o+c_t}\; k_o \alpha q I$$

$$= q\, S_{wing}\, \alpha\, \frac{2k_o}{1+TR}\; I$$

$$\equiv C_{L_\alpha}\, q\, S_{wing}\, \alpha$$

from which one obtains

$$C_{N_\alpha} \simeq C_{L_\alpha} = \frac{2k_o}{1+TR}\; I$$

An important parameter, which is also a spanwise distribution function and will be used shortly, is

$$p(\eta) \equiv \frac{c_\ell c}{C_L c_{av}} = \frac{c_{\ell_\alpha} c}{C_{L_\alpha} c_{av}}$$

where c_{av} is the average chord. From the preceding equations, it turns out that

$$p(\eta) \equiv \frac{c_{\ell_\alpha} c}{C_{L_\alpha} c_{av}} = \frac{\sqrt{1-\eta^2}}{1-0.429\eta}\,[1+(TR-1)\eta] \left(1+a\eta^2\, \frac{\Lambda_e}{45}\right) \frac{1}{I} \qquad (22)$$

By expanding $\frac{1}{1-0.429\eta} = 1 + 0.429\eta + (0.429\eta)^2 \ . \ . \ .$, and performing the indicated integration in Eq. (21), one has also

$$I = \left(0.785398 + 0.196350a \frac{\Lambda_e}{45}\right) + (TR-0.571)\left(0.453803 + 0.197011a \frac{\Lambda_e}{45}\right) \tag{23}$$

The simple approximation Eq. (22) is the basis from which the distribution function is derived. To determine whether it is a reasonable one, its results were compared with those from the extensive parametric study reported in Reference 7. (This parametric study is based on steady-state linearized theory and covers wide ranges of M(<1), Λ, AR, and taper ratio TR.) Choosing the constant a to be equal to 1, it was found that Eq. (22) is indeed an adequate representation for (M, Λ, AR, TR)-combinations appropriate for a variety of current subsonic aircraft. It was therefore adopted.

With some algebraic manipulations, it can be shown that $g(\eta)$ is related to $p(\eta)$. From that relation, it turns out that

$$g(\eta) = \frac{1+TR}{2} \frac{\sqrt{1-\eta^2}}{1-0.429\eta} \left(1 + \eta^2 \frac{\Lambda_e}{45}\right) \frac{1}{I} \tag{24}$$

where I is according to Eq. (23) with a=1

For <u>sectional</u> lift coefficients on a 3D-wing, $\check{c}_n \equiv \check{c}_n(\eta)$, one can use

$$\frac{\check{c}_n}{c_n}(\alpha=0,\ s\to\infty) = \frac{C_N}{c_n}(\alpha=0,\ s\to\infty)\ g(\eta)$$

If one assumes that $g(\eta)$ holds at all α's (since nothing better and simple enough is available),

$$\frac{\check{c}_n}{c_n}(\alpha,\ s\to\infty) = \frac{C_N}{c_n}(\alpha,\ s\to\infty)\ g(\eta) \tag{25}$$

The distribution of the aerodynamic loading along the span as indicated by Eq. (25) is for $s\to\infty$, i.e., the steady state case. At the

other extreme of the time scale, i.e., t=s=0, three-dimensional effects should be negligible, i.e., the flow is really two-dimensional, and thus

$$\frac{\tilde{c}_n}{c_n}(\alpha,\ s=0) = 1 \tag{26}$$

In Reference 2, the following procedure is suggested for intermediate times s:

$$\left.\begin{aligned} \frac{\tilde{c}_N}{c_n}(\alpha,S) &= 1 && 0 \le s \le 1 \\ &= 1 - \left(1 - \frac{C_N}{c_n}(\alpha,\ s\to\infty)\right)\frac{s-1}{15} && 1 \le s \le 16 \\ &= \frac{C_N}{c_n}(\alpha,\ s\to\infty) && s \ge 16 \end{aligned}\right\} \tag{27}$$

(See Figure 10B of Reference 2.) With the introduction of the spanwise distribution, the following alternative to Eq. (27) is recommended to describe the variation of $\frac{\tilde{c}_n}{c_n}$ with s:

$$\left.\begin{aligned} \frac{\tilde{c}_n}{c_n}(\alpha,\ s) &= 1 && 0 \le s \le 1 \\ &= 1 - \left(1 - e^{-0.6(s-1)}\right)\left(1 - \frac{\tilde{c}_n}{c_n}(\alpha,\ s\to\infty)\right) && s \ge 1 \end{aligned}\right\} \tag{28}$$

Of course, $\frac{\tilde{c}_n}{c_n}(\alpha,\ s)$ must be multiplied by the spanwise strip width Δ_i to obtain the suitable coefficient for the strip i. The rest of the VIBRA procedure remains the same.

Based on the above discussions, the following final change and addition was made:

Change 3

(a) Find Λ_e according to Eq. (15a)

(b) Find $\xi = \frac{C_N}{c_n}(\alpha=0,\ s\to\infty)$ according to Eq. (16).

(c) Find $\frac{C_N}{c_n}(\alpha, s \to \infty)$ according to Eq. (17).

(d) Find I and $g(\eta)$ for desired η's from Eq. (23) with a = 1 and Eq. (24). Here $\eta = |2y/\tilde{s}|$.

(e) Find $\frac{\tilde{c}_n}{c_n}(\alpha, s \to \infty)$ according to Eq. (25).

This quantity will be a function of η, unlike its counterpart in earlier VIBRA versions.

(f) Find, using the results from (e) and Eq. (28), $\frac{\tilde{C}_n}{c_n}(\alpha, s)$ for desired stations η at each time s.

This change describes the recommended procedure for distributing the total leading C_N in a reasonable fashion along the span of the lifting surface.

REFERENCES

1. Hobbs, N.P., Zartarian, G., and Walsh, J.P., A Digital Computer Program for Calculating the Blast Response of Aircraft to Nuclear Explosions, Vol. I, Program Description, Air Force Weapons Laboratory Technical Report No. AFWL-TR-70-140, Vol. I, April 1971.

2. Hobbs, N.P., and Wetmore, K.R., Lethal Blast Effects of Nuclear Weapons on Selected U.S. and U.S.S.R. Aircraft, Part I - Post-Failure Structural Analysis Techniques, Unpublished.

3. Bisplinghoff, R.L., Ashley, H., and Halfman, R.L., "Aeroelasticity", Addison-Wesley Publishing Company, Inc., Reading, Mass., 1955.

4. Lomax, H., Heaslet, M.A., Fuller, F.B., and Sluder, L., Two- and Three-dimensional Unsteady Lift Problems in High-speed Flight, N.A.C.A. Report 1977, 1952.

5. Stivers, L.S., Jr., Effects of Subsonic Mach Number on the Forces and Pressure Distributions on Four NACA 64A-Series Airfoil Sections at Angles of Attack as High as 28°, NACA TN3162, March 1954.

6. Axelson, J.A., and Haacker, J.F., Subsonic Wing Loadings on a 45° Sweptback-Wing and Body Combination at High Angles of Attack, NASA Memo 1-18-59A, February 1959.

7. DeYoung, J., and Harper, C.W., Theoretical Symmetric Span Loading at Subsonic Speeds for Wings Having Arbitrary Planform, N.A.C.A. Report 921, 1948.

DISTRIBUTION LIST

DEPARTMENT OF DEFENSE

Assistant to the Secretary of Defense
Atomic Energy
ATTN: Executive Assistant

Defense Intelligence Agency
ATTN: DB-4C, V. Fratzke

Defense Nuclear Agency
ATTN: SPAS
ATTN: DDST
ATTN: STSP
4 cy ATTN: TITL

Defense Technical Information Center
12 cy ATTN: DD

Field Command
Defense Nuclear Agency
ATTN: FCPR
ATTN: FCT, W. Tyler

Field Command
Defense Nuclear Agency
Livermore Division
ATTN: FCPRL

NATO School (SHAPE)
ATTN: U.S. Documents Officer

Undersecretary of Defense for Rsch. & Engrg.
ATTN: Strategic & Space Systems (OS)

DEPARTMENT OF THE ARMY

Harry Diamond Laboratories
Department of the Army
ATTN: DELHD-N-P, J. Gwaltney
ATTN: DELHD-N-P

U.S. Army Ballistic Research Labs
ATTN: DRDAR-BLT, W. Taylor

U.S. Army Materiel Dev. & Readiness Cmd.
ATTN: DRCDE-D, L. Flynn

U.S. Army Nuclear & Chemical Agency
ATTN: Library

DEPARTMENT OF THE NAVY

Naval Material Command
ATTN: MAT 08T-22

Naval Research Laboratory
ATTN: Code 2627

Naval Surface Weapons Center
ATTN: Code F31, K. Caudle

Naval Weapons Evaluation Facility
ATTN: L. Oliver

Office of Naval Research
ATTN: Code 465

DEPARTMENT OF THE NAVY (Continued)

Strategic Systems Project Office
Department of the Navy
ATTN: NSP-272

DEPARTMENT OF THE AIR FORCE

Aeronautical Systems Division
Air Force Systems Command
ATTN: ASD/ENFT, R. Bachman
4 cy ATTN: ASD/ENFTV, D. Ward

Air Force Aero-Propulsion Laboratory
ATTN: TBC, M. Stibich

Air Force Materials Laboratory
ATTN: MBE, G. Schmitt

Air Force Weapons Laboratory, AFSC
ATTN: DYV, A. Sharp
ATTN: SUL
ATTN: DYV, G. Campbell

Assistant Chief of Staff
Studies & Analyses
Department of the Air Force
ATTN: AF/SASB, O. Ramlo
ATTN: AF/SASC, B. Adams

Deputy Chief of Staff
Research, Development, & Acq.
Department of the Air Force
ATTN: AFRDQSM, L. Montulli

Foreign Technology Division
Air Force Systems Command
ATTN: SDBF, S. Spring

Strategic Air Command
Department of the Air Force
ATTN: XPFS, F. Tedesco
ATTN: XPFS, B. Stephan

DEPARTMENT OF ENERGY CONTRACTOR

Sandia Laboratories
ATTN: Document Control for A. Lieber

DEPARTMENT OF DEFENSE CONTRACTORS

AVCO Research & Systems Group
ATTN: P. Grady
ATTN: J. Patrick

BDM Corp.
ATTN: C. Somers

Boeing Co.
ATTN: E. York
ATTN: R. Dyrdahl
ATTN: S. Strack

Boeing Wichita Co.
ATTN: R. Syring
ATTN: K. Rogers

DEPARTMENT OF DEFENSE CONTRACTORS (Continued)

Capspan Corp.
ATTN: M. Dunn

University of Dayton
ATTN: B. Wilt

Effects Technology, Inc.
ATTN: R. Globus
ATTN: R. Parisse
ATTN: R. Wengler
ATTN: E. Bick

General Electric Company-TEMPO
ATTN: DASIAC

General Research Corp.
ATTN: T. Stathacopoulos

Kaman AviDyne
ATTN: E. Criscione
ATTN: N. Hobbs
ATTN: R. Ruetenik
ATTN: B. Lee
ATTN: G. Zartarian

Kaman Sciences Corp.
ATTN: D. Sachs

DEPARTMENT OF DEFENSE CONTRACTORS (Continued)

Los Alamos Technical Associates, Inc.
ATTN: C. Sparling
ATTN: P. Hughes

McDonnell Douglas Corp.
ATTN: J. McGrew

Prototype Development Associates, Inc.
ATTN: C. Thacker
ATTN: H. Moody
ATTN: J. McDonald

R & D Associates
ATTN: A. Kuly
ATTN: C. MacDonald
ATTN: J. Carpenter
ATTN: F. Field

Rockwell International Corp.
ATTN: R. Moonan

Science Applications, Inc.
ATTN: J. Dishon